

Article

Effect of Copper on Microstructure and Corrosion Resistance of Hot Rolled 301 Stainless Steel

Na Li ^{1,*} , Hangxin Yan ¹, Xuyuan Wang ¹, Lei Xia ¹ , Yuchuan Zhu ¹, Yan Li ² and Zhengyi Jiang ^{3,*}¹ School of Materials and Metallurgy, University of Science and Technology Liaoning, Anshan 114051, China² State Key Laboratory of Metal Material for Marine Equipment and Application, Iron & Steel Research Institutes of Ansteel Group Corporation, Anshan 114009, China³ School of Mechanical, Materials, Mechatronic and Biomedical Engineering, University of Wollongong, Wollongong, NSW 2522, Australia

* Correspondence: lina@ustl.edu.cn (N.L.); jiang@uow.edu.au (Z.J.)

Abstract: The effect of copper (Cu) on hot-rolled 301 austenitic stainless steel (ASS) was studied by observing the microstructures and testing the electrochemical corrosion resistance properties. The results showed that, with the increase in Cu content, the size of shear zones in 301 ASS decreased, and the number increased, which increased the uniformity of the microstructure macroscopically. The presence of Cu decreased the stacking fault energy of 301 ASS at elevated temperatures. Meanwhile, the amount of chromium (Cr) carbides decreased gradually with the increase in Cu content, which implies that the solid solution of Cu in hot-rolled 301 stainless steel promotes the solid solution of Cr and C in the steel, which is conducive to the formation of Cr-rich passivation films. As a result, the corrosion resistance of hot rolled Cu-bearing 301 stainless steel is improved, with both lower corrosion current density (I_{corr}) and passivation current (I_{pass}), and more positive corrosion potentials (E_{corr}) and passivation potential (E_p), even though it does not show a higher pitting resistance. As Cu content in the steel was increased from 0.4% to 1.1%, the corrosion resistance was not further improved.

Keywords: 301 austenitic stainless steel; copper; hot-rolled microstructure; stacking fault energy; corrosion resistance



Citation: Li, N.; Yan, H.; Wang, X.; Xia, L.; Zhu, Y.; Li, Y.; Jiang, Z. Effect of Copper on Microstructure and Corrosion Resistance of Hot Rolled 301 Stainless Steel. *Metals* **2023**, *13*, 170. <https://doi.org/10.3390/met13010170>

Academic Editor: Krzysztof Rokosz

Received: 22 December 2022

Revised: 5 January 2023

Accepted: 10 January 2023

Published: 14 January 2023



Copyright: © 2023 by the authors. Licensee MDPI, Basel, Switzerland. This article is an open access article distributed under the terms and conditions of the Creative Commons Attribution (CC BY) license (<https://creativecommons.org/licenses/by/4.0/>).

1. Introduction

Stainless steel is marked as a sustainable construction material, which has excellent corrosion resistance and durability, thus leading to low maintenance and inspection costs during its service life, and is 100% recyclable after use. With the advancement in metallurgical and manufacturing techniques, the direct hot rolling of stainless-steel products has become possible [1,2] because of its great corrosion resistance and favourable mechanical properties, including high strength and excellent ductility [3,4].

Single-phase 301 ASS has a low yield ratio, good plastic processing performance, and high corrosion resistance under atmospheric conditions. Compared with the widely reported 304 steel, 301 steel has a higher C content and lower Cr and Ni contents and is suitable for a variety of situations requiring high strength. However, its corrosion resistance is poor under acid, alkali, and salt conditions [5,6]. Therefore, one of the purposes of this study is to improve the corrosion resistance of 301 ASS, improve its comprehensive performance, and expand its application range by adding an appropriate amount of Cu.

On the other hand, when scrap steel is reused, copper accumulates in the steel because it is difficult to remove in the steelmaking process. Therefore, with the increase in scrap steel, it is imperative to study the application of copper in steels. In addition to Cu-bearing weathering steel and antibacterial stainless steel, it is necessary to systematically develop the research and application of copper in steel. Much research has been undertaken on the effect of Cu on the microstructure and properties of steels [7–10]. Some results generally

show that adding an appropriate amount of Cu to stainless steels can significantly improve corrosion resistance in a variety of environments [11–15].

At present, there are few reports on the effect of Cu on the microstructure and corrosion resistance of hot-rolled stainless steels. In this paper, different contents of Cu were added to 301 ASS, the microstructures of hot-rolled 301 ASS containing Cu were systematically observed, and the electrochemical corrosion resistance of the steels was tested and analysed.

2. Experimental Materials and Methods

301 ASS was used as the raw material, around 0.5 wt.% and 1.0 wt.% Cu were added to the steel, respectively, because copper has a cumulative effect in the process of scrap recycling, and it is not appropriate to add too much Cu intentionally, and excessive Cu will cause Cu brittleness. The experimental steels were vacuum-melted and cast into 25 kg cylindrical ingots with a diameter of \varnothing 150 mm. Plates with a thickness of 12 mm were obtained after the steel was heated at 1200 °C for 1 h and hot rolled for 5 passes. The spectral test results of the experimental steels' compositions are shown in Table 1.

Table 1. Chemical composition of test 301 stainless steels/(wt.%).

Sample No.	C	Cr	Ni	Mn	Cu	Si	Fe
301ASS	0.104	16.069	6.018	1.295	0.009	0.370	Bal
301ASS-0.4Cu	0.091	16.800	6.460	1.050	0.443	0.400	Bal
301ASS-1.1Cu	0.119	16.378	6.194	1.388	1.090	0.381	Bal

The hot-rolled steel plates were machined into samples with the size of 10 mm \times 10 mm \times 12 mm by a wire-cutting method. Rolling directions were marked during cutting. A metallographic microscope (VHX-5000, Keyence, Osaka, Japan) and a scanning electron microscope (SEM Sigma500, ZEISS, Oberkochen, German), equipped with energy spectrum, were used to observe the microstructures and test the compositions. Microhardness tests (with Q10, Qness, Golling an der Salzach, Austria) were carried out directly with the observed samples.

A 10 mm \times 10 mm working surface was reserved after the sample was polished, and all other surfaces were sealed with epoxy resin. The Autolab electrochemical workstation (PGSTAT302N, Metrohm Autolab, Herisau, Switzerland) was used to measure the corrosion resistance of the test steel with a three-electrode system, where Ag/AgCl/sat.KCl was used as the reference electrode, Pt was used as the auxiliary electrode, and the working current was applied to the experimental steel samples. The working temperature was maintained at 25 °C. Before the experiment, the working electrode surface was degreased with acetone and then rinsed with deionised water, and a 3.5% sodium chloride solution with a pH value of 6.5–7.0 was used at 25 °C. Potentiodynamic polarisations were conducted from a potential of -0.8 V to 0.6 V versus Ag/AgCl with a scan rate of 0.05 V/min after achieving a stationary value for the open circuit potential (potential variation not higher than 0.1 mV/s).

3. Results and Analysis

3.1. Hot Rolled Microstructure

Figure 1 shows the metallographic hot-rolled microstructures of the 301 stainless steels with different Cu contents. There were some strip-shaped shear zones (pointed to by arrows in Figure 1) along the rolling direction in the steel. As the Cu content increases in the steels, the size of the shear zones decreases, but the number increases sequentially, which leads to an increase in the overall uniformity of the deformed microstructure.

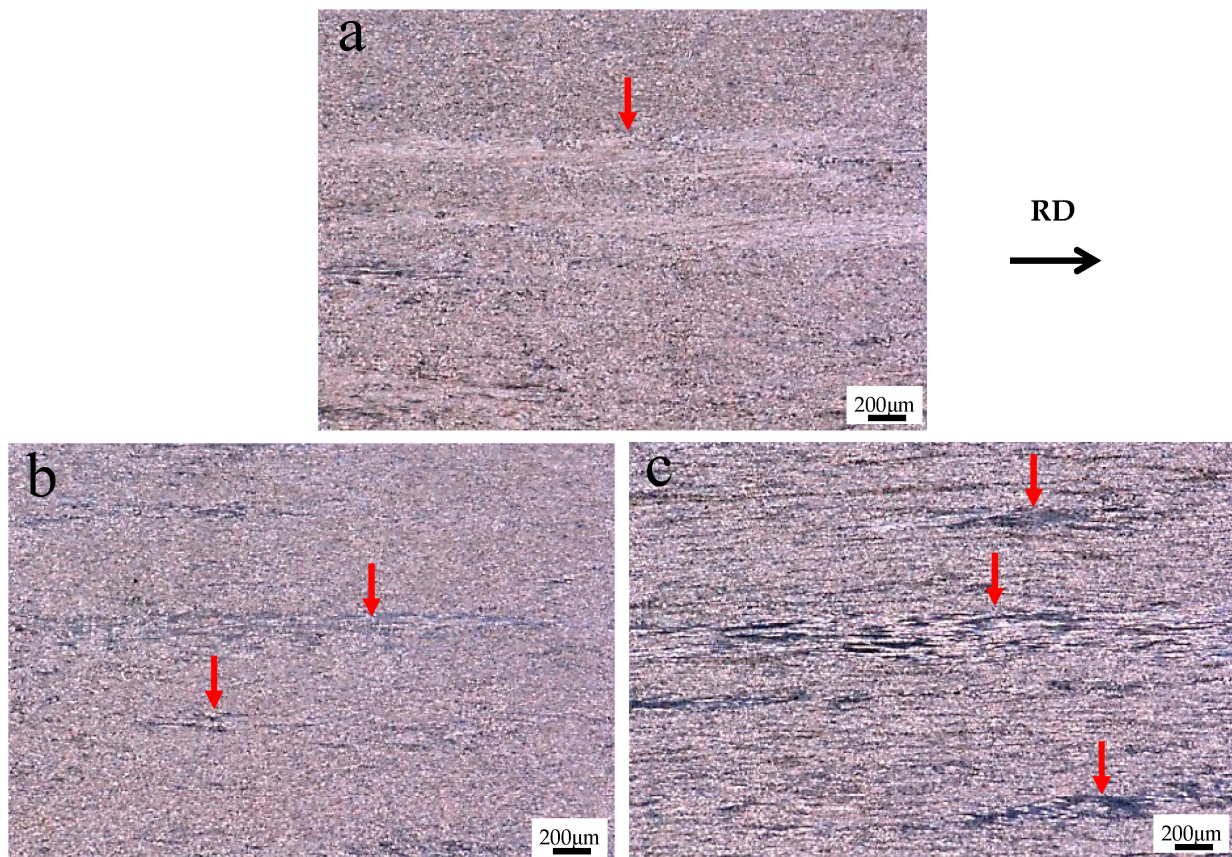


Figure 1. Microstructures of hot-rolled 301 ASS ((a): 301ASS, (b): 301ASS-0.4Cu, (c): 301ASS-1.1Cu).

The shear bands and nearby microstructures of 301ASS-1.1Cu were further observed, as shown in Figure 2. Enlarged photos of area 1 and area 2 in Figure 2a are shown in Figure 2b and Figure 2c, respectively. Comparing Figure 2b and Figure 2c, it can be seen that the austenite grains around the shear band displayed significant recovery and recrystallisation, but they did not appear in the shear band. Hou et al. [16] report that shear bands are formed due to severe local deformation in the steel.

During the process of high-temperature deformation, 301 stainless steel coexists in two phases: ferrite and austenite [17]. The two phases will produce deformation differences due to the different lattice structures, resulting in nonuniform local deformation between the two phases. In addition, the local nonuniform deformation may also be related to temperature conduction, which is caused by the local inhomogeneous temperature. However, the shear bands become smaller and more numerous, and are evenly distributed, which also reflects the homogeneity of the microstructure in the macro view.

It is well known that copper can enlarge the austenitic phase region in steel, so it will affect the proportion of ferrite and austenite at high temperatures, and then affect the deformation of the two phases and interphases. At the same time, the solution of copper in steel may also affect the temperature conduction in steel, thus affecting the temperature distribution during the deformation process. According to the distribution of shear bands in Figure 1, the overall deformation of steels with higher copper content tends to be more uniform. Therefore, the macroscopic shear bands in Figures 1 and 2 are related to discontinuous local plastic deformation and/or uneven temperature distribution in the hot rolling process [17].

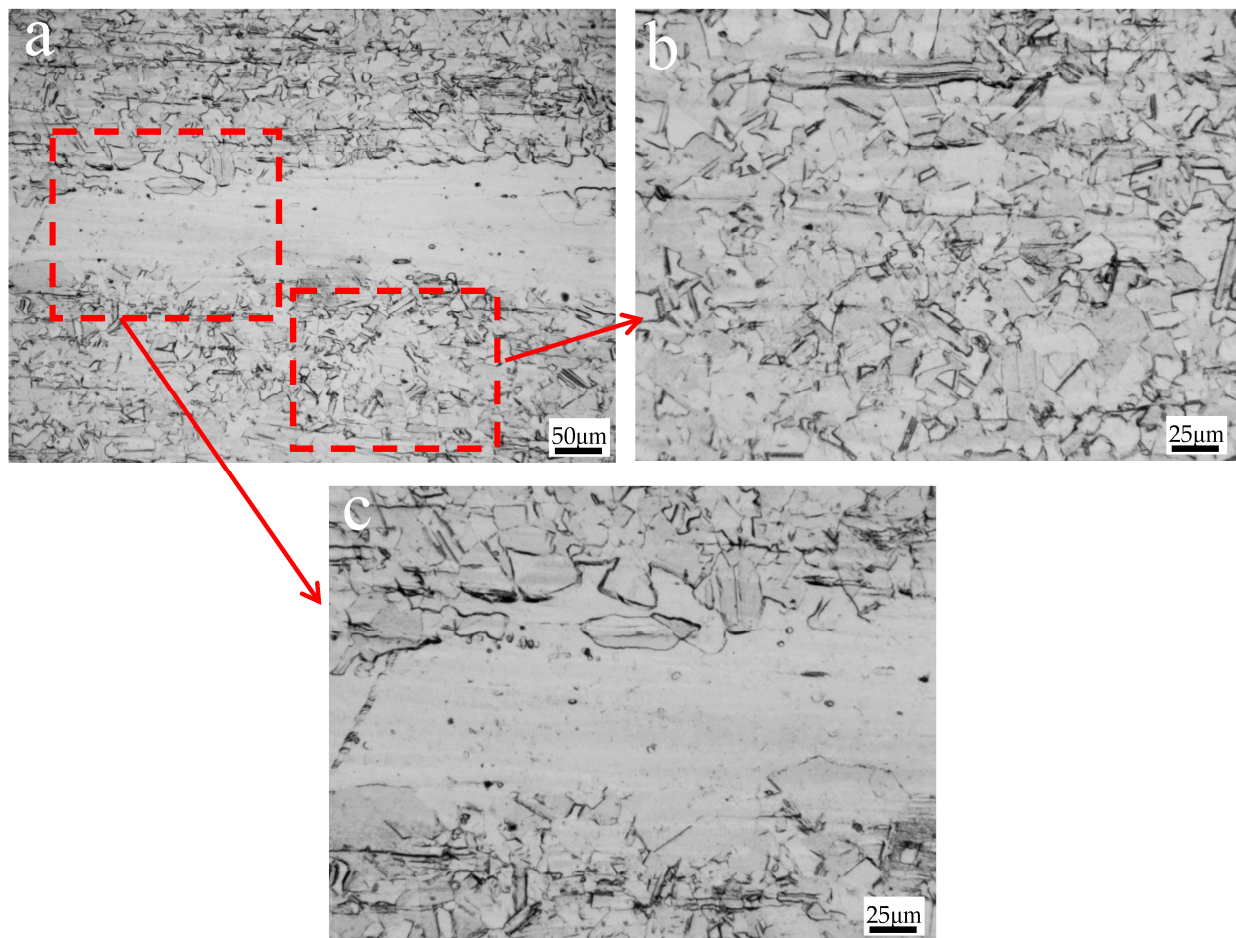


Figure 2. Metallographic photographs of shear band (a,c) and surrounding recrystallized microstructures (b) of 301ASS-1.1Cu.

It can be seen from Figure 1 that the number of shear bands of the experimental steel increases with the increase in Cu content, and their distribution becomes more uniform. The more uniform the distribution of shear bands in the steel, the more uniform the macrostructure of the steel. Therefore, the addition of Cu affects the coordination of deformation and/or the thermal conductivity properties of the steel in the hot rolling process and promotes the uniformity of the overall microstructure by affecting deformation and heat transfer [17,18].

3.2. Recrystallised Microstructure

Figure 3 shows the metallographic microstructures in the complete recrystallisation region of hot-rolled 301 stainless steels with different Cu contents. The austenitic grain size in Figure 3 is measured by using the transactional method; that is, drawing several straight lines on the figure, measuring the length of the straight line with reference to the ruler, and counting the number of grains along the straight line, so as to obtain the statistical size of the grains. The grain sizes of 301ASS, 301ass-0.4Cu and 301ass-1.1Cu are 6.43 μm , 6.12 μm , and 5.75 μm , respectively. Therefore, grain size decreases with the increased copper content in the steel.

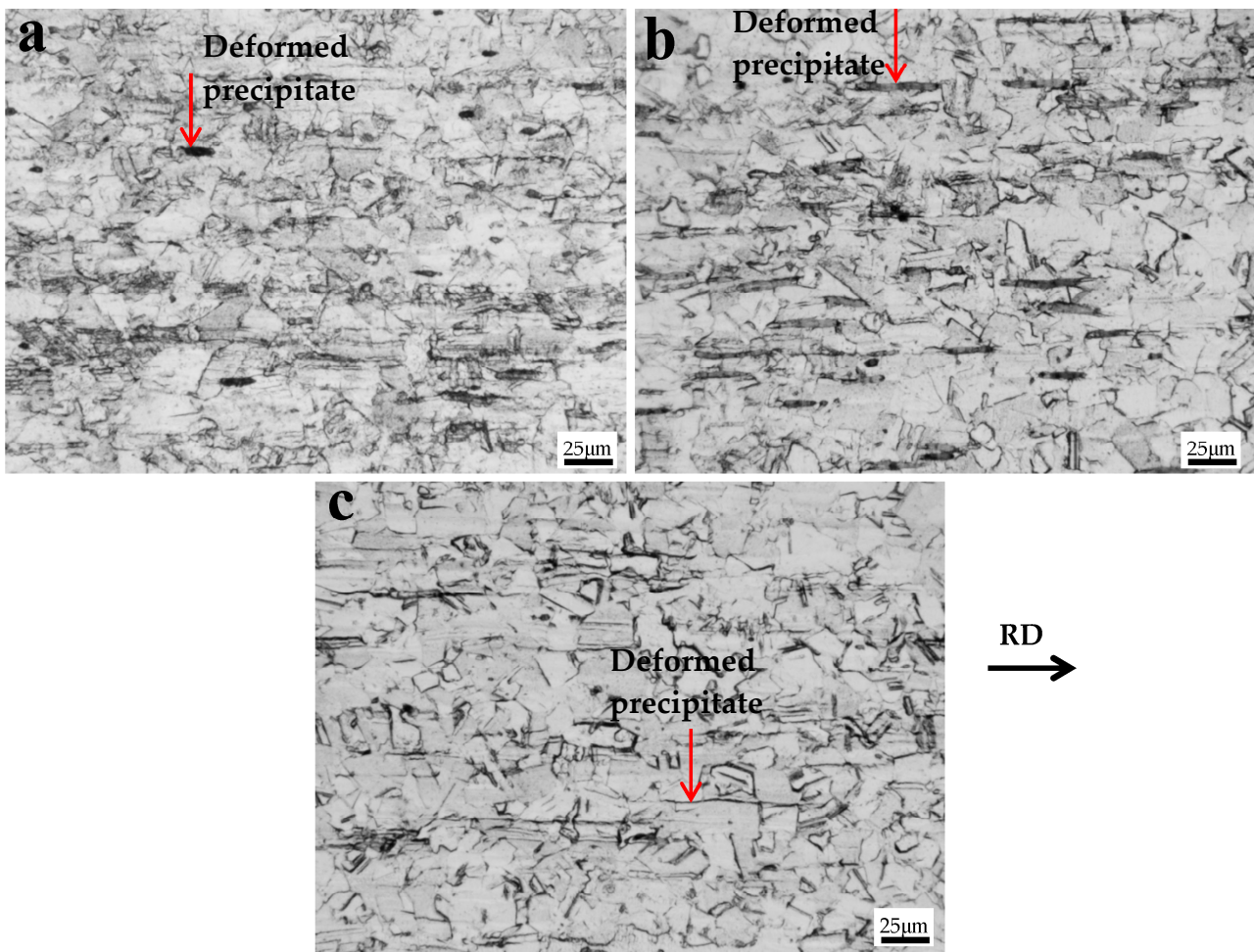


Figure 3. Metallographic photos of the recrystallised area of each experimental steel sample with different Cu content ((a): 301ASS, (b): 301ASS-0.4Cu, (c): 301ASS-1.1Cu).

It can be seen from Figure 3 that there are many randomly distributed black banded “precipitates” along the rolling direction (pointed to by arrows in Figure 3). In Figure 3a, although the precipitates are small and dispersed, they are still elongated along the rolling direction. The number of banded precipitates decreases, and the length increases when the Cu content is about 0.4%. With the continuous increase in copper content, the precipitates become obviously finer. Further observation of these precipitates with SEM shows that the precipitates in Figure 3 are actually some pits, and the actual phase has fallen off, as shown in Figure 4.

Figure 4 shows the SEM photo (SE1) of 301ASS-0.4Cu and the surface scan photos of the main alloying elements. After etching the sample with aqua regia, small band-like pits can be easily observed in the secondary electron morphology in Figure 4. It can be judged that the precipitated phases corresponding to the shape of the pits were etched away. The composition spectra of the alloying elements C, Cr, Mn, Ni, and Fe were scanned, the distribution of all the elements at the corresponding positions of pits in the secondary electron image is relatively uniform, and there is no obvious segregation, indicating that the particles have fallen off.

Since the banded structures could not be detected when the sample was etched, the microstructures of the unetched samples were observed, and the compositions were tested, respectively, with SEM, as shown in Figure 5.

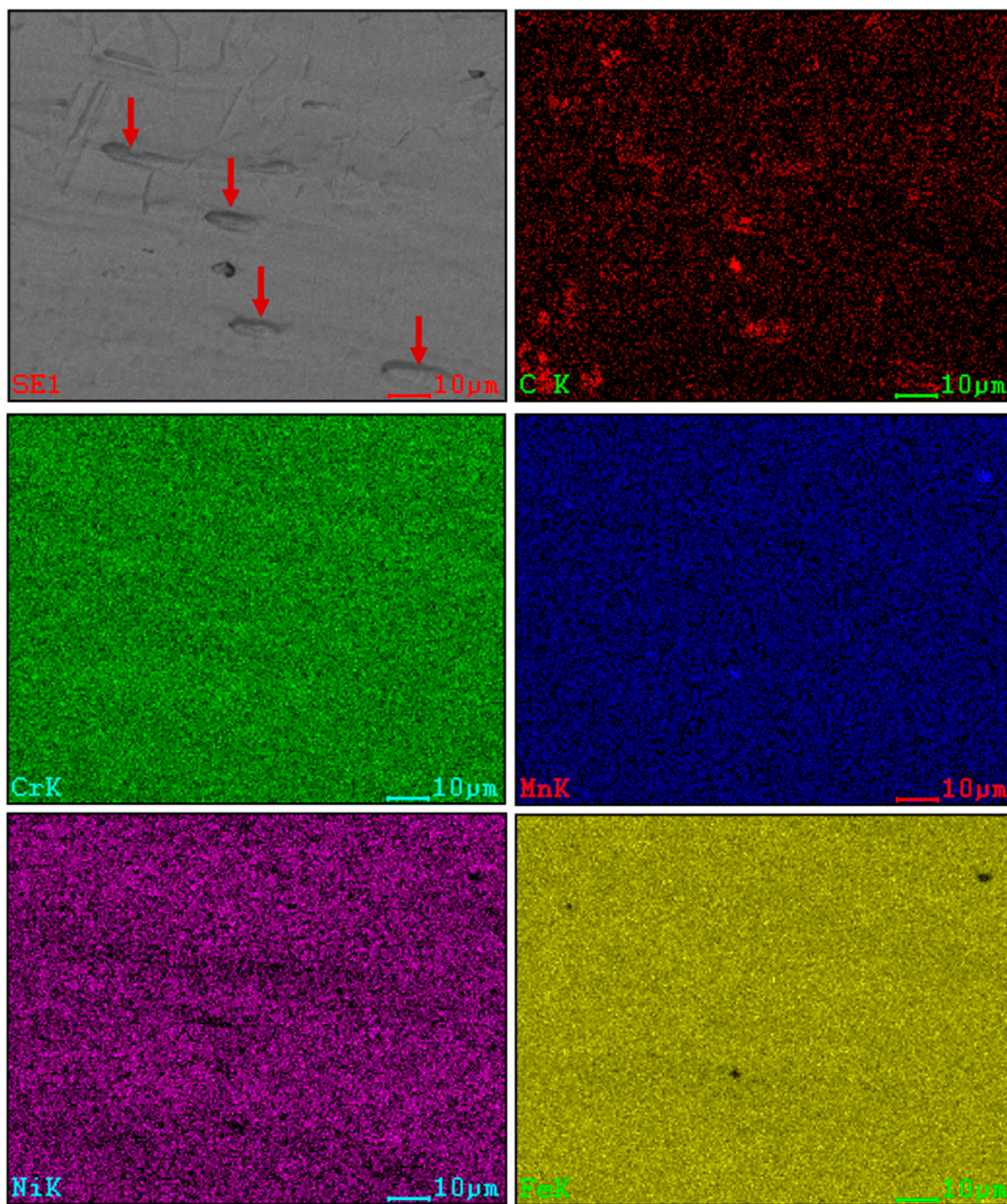


Figure 4. SEM photo of etched 301ASS-0.4Cu and surface scan photos of the main alloying elements.

Figure 5 shows the SEM photograph of unetched 301ASS-0.4Cu and the surface scanning photograph of the main alloying elements C, Cr, Mn, Ni, and Fe. Although the sample was not etched, banded structures could be identified by SEM, as indicated by the arrows in Figure 5. The Cr content in the corresponding positions of the banded structures is significantly higher than that in the surrounding area (shown by arrows in Figure 5). At the same time, the content of Ni in the corresponding position is lower, indicating that the banded structure should be a Cr-rich phase and poor in Ni. Meanwhile, the distribution of Mn and Fe is relatively uniform, and there is no obvious aggregation. Cr is a strong carbide-forming element [19]; therefore, it is inferred that the banded structure is chromium carbide. There is no obvious C aggregation in Figure 5 because the energy spectrum of SEM is not sensitive to light elements such as C. In addition, it is easy to introduce impurities during the sample's preparation, which affects the surface content of C and other elements. Chromium carbides chemically reacted with aqua regia during the etching process and were etched away, leaving only banded pits, as shown in Figure 4.

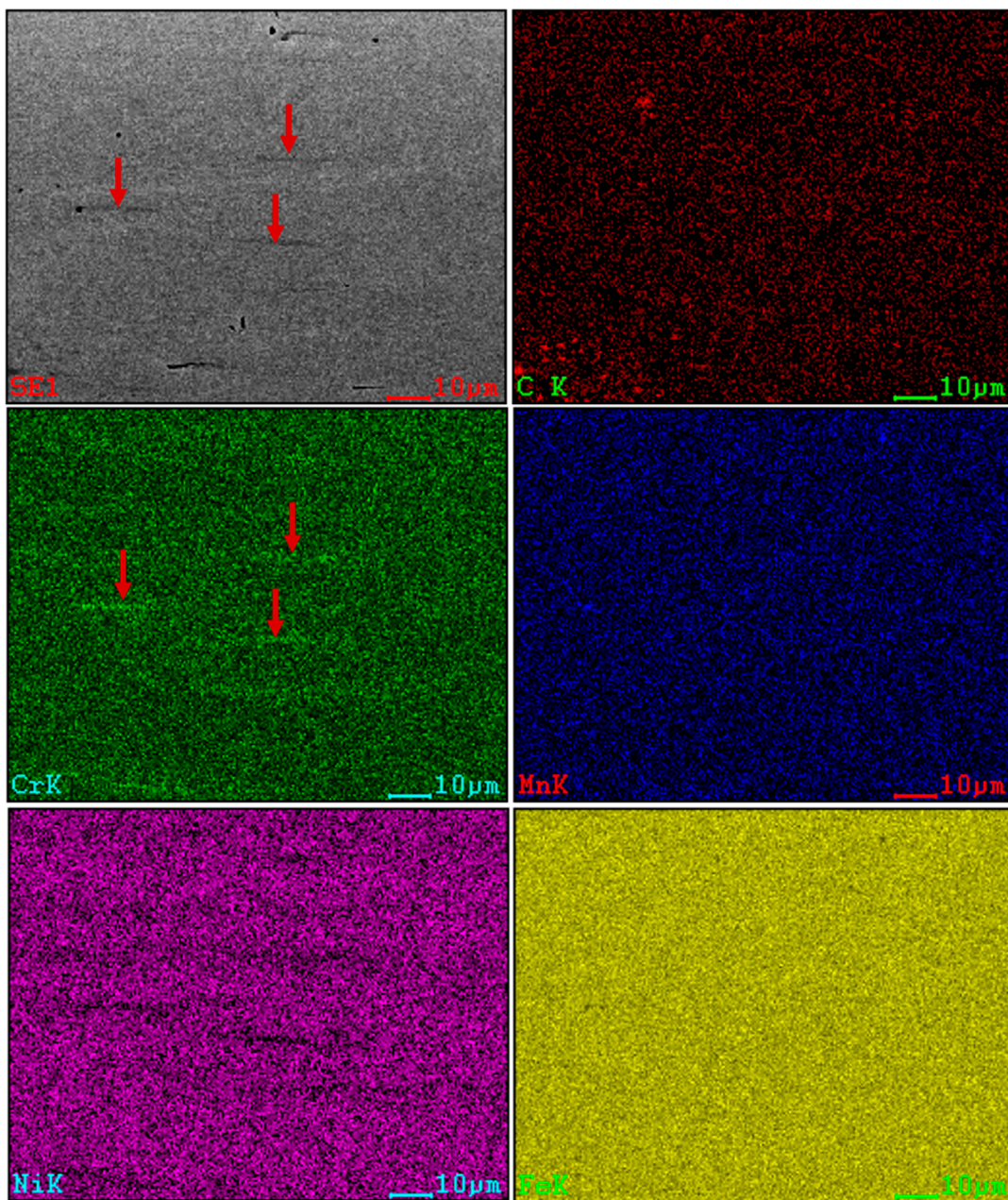


Figure 5. SEM photo of unetched 301ASS-0.4Cu and the surface scan photos of main alloying elements.

According to the above results and analysis, it can be judged that the banded structures in each sample microstructure in Figure 3 are mainly chromium carbides. Obviously, plastic deformation occurred with these carbides along the rolling direction, according to Figure 3. Carbides are usually brittle particles, and among various carbides containing chromium, $(\text{Fe, Cr})_7\text{C}_3$ can undergo a certain degree of plastic deformation [20]; therefore, this carbide should be $(\text{Fe, Cr})_7\text{C}_3$.

As the Cu content increased in the steels, the amount of $(\text{Fe, Cr})_7\text{C}_3$ decreased gradually, which indicates that the solid solubility of Cr and C increased in the steels. Both the solid solution and precipitation of Cu in Cu-bearing steels will cause lattice distortion to a certain extent, which should be beneficial to the solid solution of Cr and C atoms in steel, so the amount of $(\text{Fe, Cr})_7\text{C}_3$ decreases.

In Figures 4 and 5, some small Mn-rich precipitates can also be observed, which are poor in Fe, small in size ($\leq 2 \mu\text{m}$), and will not deform along the rolling direction, so they can be inferred to be MnS [21].

Figure 6 shows SEM photos of the recrystallised microstructure of hot-rolled 301 stainless steels with different Cu contents. It can be seen from Figure 6 that with the increase in Cu content, the number of precipitates (pits) in the steel gradually decreased, and the degree of disorder in the grains decreased as well.

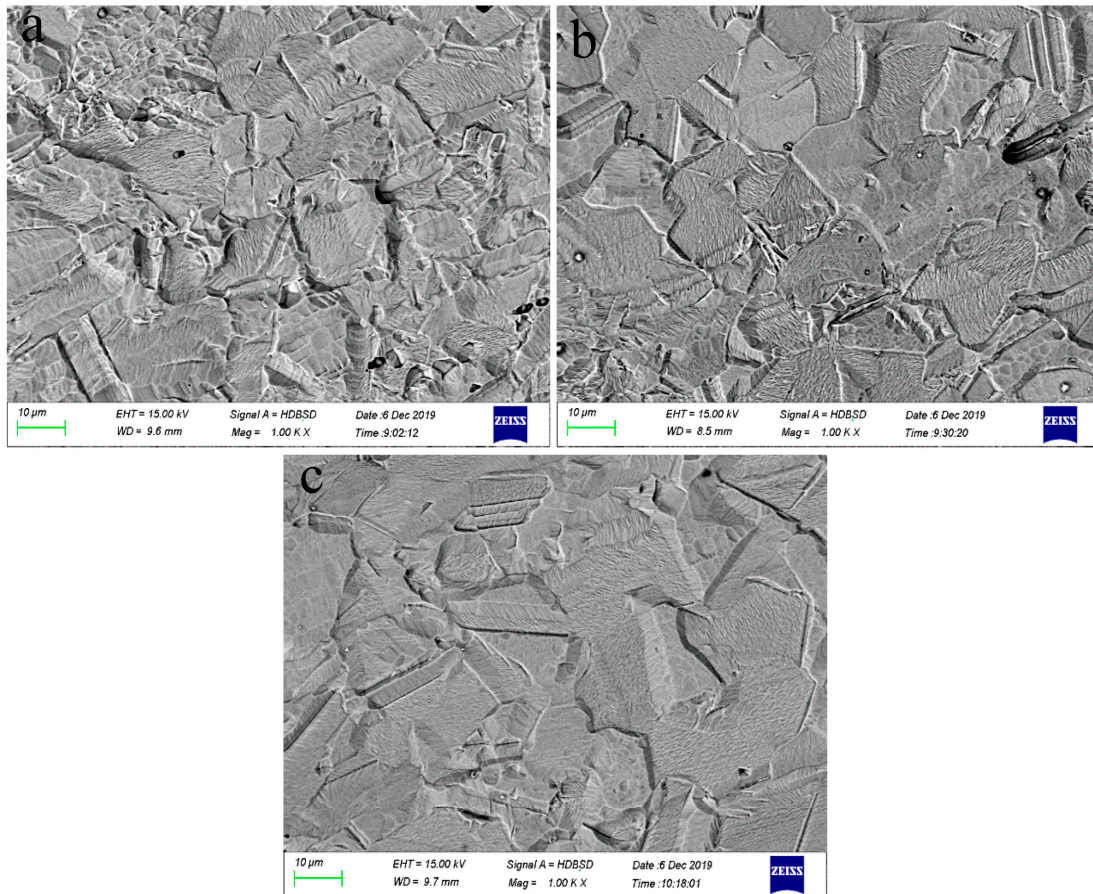


Figure 6. SEM pictures of recrystallisation areas of stainless steel samples with different Cu content ((a): 301ASS, (b): 301ASS-0.4Cu, (c): 301ASS-1.1Cu).

Hot-rolled deformation can be coordinated by dislocation glide and twinning. Figure 6 shows that with the increase in Cu in the steel, the dislocation glide in the grains became less and less, while the amount of twinning increased. It has been recognised that plastic deformation is mainly realised by martensitic transformations at low stacking fault energy (γ_{SFE}) values and by twinning at intermediate γ_{SFE} values ($18 \lesssim \gamma_{\text{SFE}} \lesssim 45 \text{ mJ m}^{-2}$). At high γ_{SFE} values ($\gtrsim 45 \text{ mJ m}^{-2}$), plasticity and strain hardening are controlled solely by dislocation glide [22]. Therefore, the γ_{SFE} decreased with increasing Cu content in hot-rolled 301 stainless steels, according to Figure 6.

It is well known that both Ni and Cu can increase the stacking fault energy of austenite steel, stabilise austenite, and inhibit martensite transformation at ambient temperature [23–25]. However, Dong et al. [26] have investigated the impact of Ni on γ_{SFE} in austenitic stainless steel as a function of temperature using first principles alloy theory. The influence of Ni on γ_{SFE} has been demonstrated to strongly depend on temperature and can become completely opposite to the one well established at ambient temperature. Therefore, it is reasonable that Cu tends to decrease γ_{SFE} at elevated temperatures and shows an enhanced effect with the increase in Cu content in the hot rolling process.

In the hot rolling process, the grains are deformed and broken to varying degrees, and more defects, such as vacancies, dislocations, twins, and small-angle grain boundaries, will appear in the grains, thus increasing the solid solution amount of Cu [10,27], Cr and

other elements. According to Figures 3 and 6, with increased Cu content in the steel, the amount of chromium carbide decreased, and the amount of twinning increased, indicating the increased solid solution of Cu, Cr, and C.

3.3. Microhardness

The microhardness (HV1) results are $202.4 (\pm 7.0)$, $175.2 (\pm 3.5)$, and $202.8 (\pm 5.0)$ for hot-rolled 301ASS, 301ASS-0.4Cu, and 301ASS-1.1Cu, respectively. The microhardness of hot-rolled Cu-bearing 301 ASS showed a slight decreasing trend, which was believed to be the result of the synergistic effect of the softening effect caused by the change in SFE and the solid solution strengthening effect [28] caused by the addition of Cu. The replacement solid solution will be formed when Cu is added to steel, but the atomic radii of Cu and γ -Fe have very small difference, being 0.128 nm and 0.124 nm, respectively. Therefore, the lattice dislocation caused by the replacement of Cu atoms with γ -Fe atoms is very small, which leads to a slight change in the lattice constant, resulting in a slight solid solution strengthening effect.

3.4. Corrosion Resistance

Figure 7 shows the polarisation curves of 301 ASS with different Cu content measured in 3.5 wt.% NaCl solution. Table 2 shows the fitting results of the polarisation curves in Figure 7. It can be seen that the corrosion current densities (I_{corr}) of the two Cu-bearing 301ASS steels are lower than that of basic 301ASS, and the corrosion potentials (E_{corr}) are slightly more positive as well, which shows the same trend that the corrosion resistance of hot rolled 301 stainless steel is improved by the addition of Cu. Both corrosion potential and corrosion current density show a small difference between 301ASS-0.4Cu and 301ASS-1.1Cu.

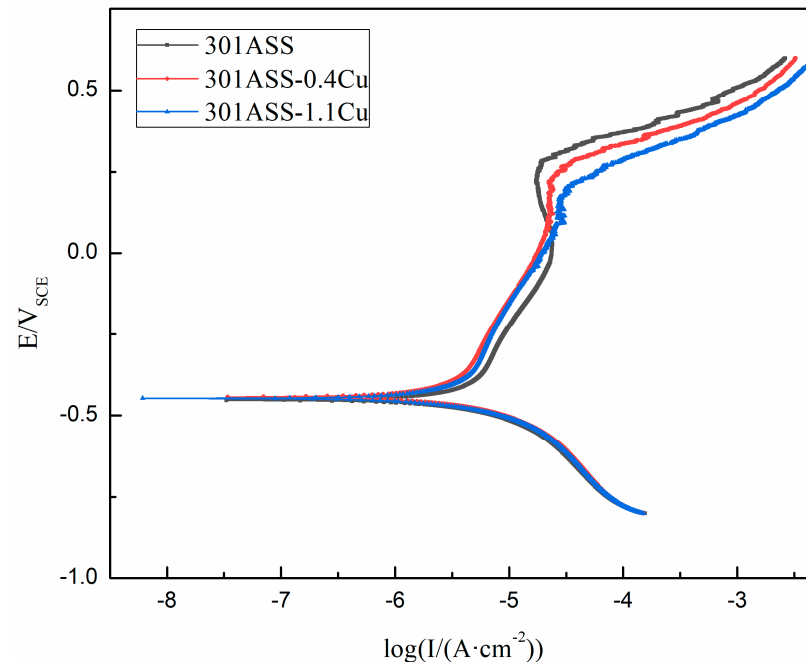


Figure 7. Polarisation curves of Cu-bearing 301 ASS in 3.5 wt.% NaCl solution.

Table 2. Electrochemical parameters of Cu-bearing 301 ASS.

Specimen	I_{corr} /($A \cdot cm^{-2}$)	E_{corr} /(V_{SCE})	E_p/V	I_{pass} /($A \cdot cm^{-2}$)	E_b/V	$v/(g \cdot m^{-2} \cdot h^{-1})$
301ASS	3.707×10^{-6}	-0.453	-0.333	6.761×10^{-6}	0.283	0.026
301ASS-0.4Cu	2.626×10^{-6}	-0.443	-0.323	5.093×10^{-6}	0.218	0.018
301ASS-1.1Cu	2.999×10^{-6}	-0.448	-0.328	5.521×10^{-6}	0.169	0.021

Meanwhile, both passivation potential (E_p) and passivation current (I_{pass}) show the same tendency, which makes it clear that the protection and stability of the passivation film of Cu-bearing 301ASS have been improved, showing a better corrosion resistance. Therefore, hot-rolled 301ASS containing Cu is not prone to corrosion, and once corroded, its corrosion rate is relatively low. Although the observed differences in corrosion properties are small, the results of several experiments are clearly consistent. Ujiro et al. [12] explained the effect of alloying Cu (~0.5 wt.%) on the corrosion resistance of stainless steels in chloride media for austenitic stainless steels; they believed that alloying Cu showed a beneficial effect in an active potential range because of the stability of deposited Cu on an anodic surface. Hermas et al. [13] also observed that the addition of 2% Cu in 304 austenitic stainless steel decreased the corrosion and critical current densities sharply because of the presence of insoluble cuprous chloride (CuCl) dispersed on the steel surface in deaerated dilute acidic chloride (Cl^-) solutions at 30 °C and 60 °C. Therefore, adding an appropriate amount of Cu to 301 stainless steel can steadily improve the corrosion resistance of the steel. While, with the increase in Cu content in the steel, the corrosion resistance of the steel has not been further improved, according to Figure 7 and Table 2.

With the increase in potential, the stability of the passivation film decreases gradually, resulting in a gradual increase in current density at the end of the passivation region. The passivation region of Cu-bearing steels is narrow, and no obvious secondary passivation occurs, and their pitting potential (E_b) is lower, indicating a poor pitting resistance.

Figure 8 shows the morphology of the protective film on the steel surface of 301ASS and 301ASS-0.4Cu and the scanning of the main elements. It can be seen from Figure 8 that, by adding 0.4% Cu, the Cr-rich protective layer on the steel surface is thicker and more continuous, but no copper enrichment was observed on the steel surface. Sample 301ASS-1.1Cu shows the same results as 301ASS-0.4Cu.

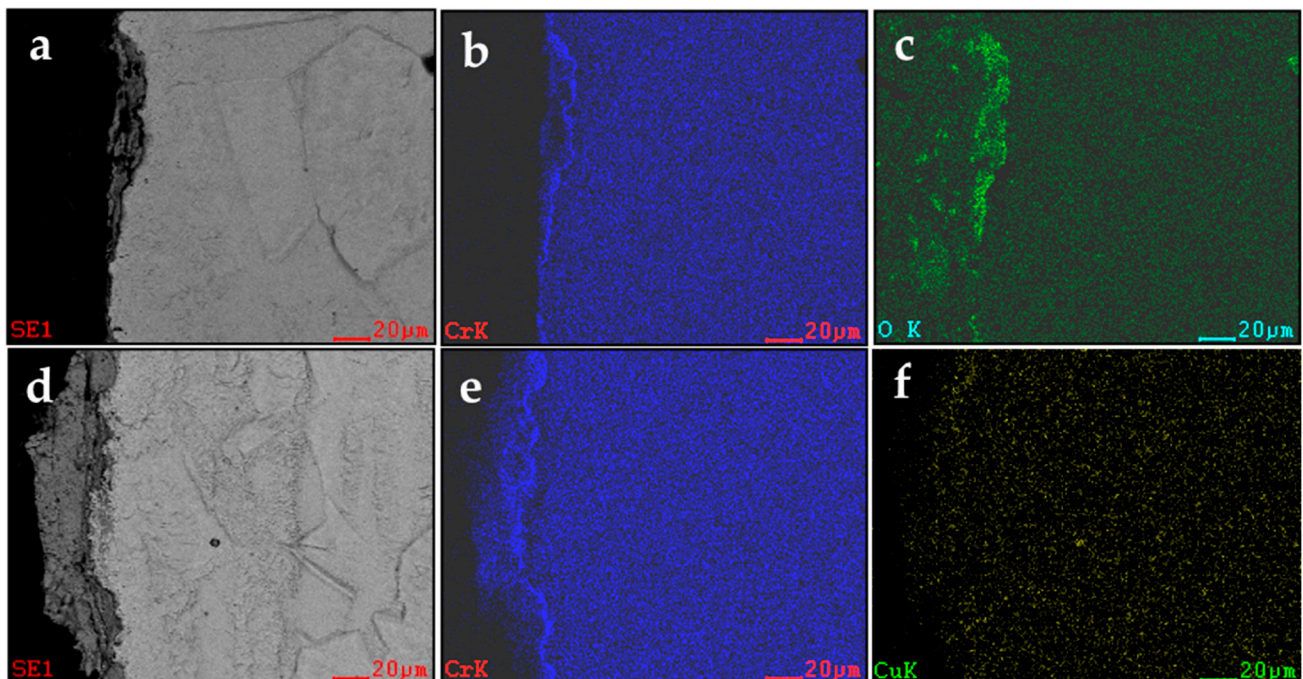


Figure 8. SEM photo of the protective film on the steel surface and the scanning of main elements: (a–c) for 301 ASS and (d–f) for 301ASS-0.4Cu.

Oguzie et al. [11] reported that Cu addition in austenitic stainless steels generally improved corrosion resistance and facilitated passivation by increasing the donor and acceptor densities. This may be related to the solid solution of alloy elements in the steel. Adding an appropriate amount of Cu to super austenitic stainless steel is conducive to the formation of a Cu-containing passivation film and improving the stability of the passivation

film in the corrosion process [15]. At the same time, both the thickness and continuity of the Cr and Mo oxide layer in the sample containing Cu are better [15]. Therefore, the formation of a Cr-rich passivation film is related to the solid solution of Cu and Cr in stainless steel.

Hot-rolled 301 stainless steel has experienced heating and deformation at high temperatures. In this process, Cu mainly exists in a solid solution state because Cu has no time and opportunity to precipitate. At the same time, the solid solution of Cu, Cr, and C increases gradually with the increase in Cu in the steel, according to the microstructure observation. Therefore, the increased solid solution of both Cu and Cr results in improved corrosion resistance in hot-rolled 301 ASS.

However, the excessive Cu content in steel, or the enrichment of Cu due to the consumption of iron and other elements in the corrosion process, will also lead to the precipitation of a Cu-rich phase in the passivation film, which will affect the continuity of the film [11] and degrade the pitting performance of the steel.

4. Conclusions

In this paper, the microstructures of hot-rolled Cu-bearing 301 ASS were systematically observed, its electrochemical corrosion properties were tested, and the following conclusions were obtained:

1. With the increase in Cu content, the shear bands in hot-rolled 301 ASS decreased in size, increased in quantity, and were distributed uniformly, which promoted the uniformity of the deformed microstructure in macro view.

2. With the increase in Cu content in 301 ASS, the dislocation in the deformed microstructure decreased gradually, and more twins appeared, indicating that Cu reduced the stacking fault energy of 301 ASS at elevated temperatures. At the same time, the amount of Cr carbide ((Fe, Cr)₇C₃) in steel decreased with the increase in Cu content, so the addition of copper promotes the solid solution of Cu, Cr, and C in steel.

3. Cu promoted the solid solution of Cr in hot-rolled 301 ASS, thus making the Cr-rich protective layer on the steel surface thicker and more continuous, thus improving the corrosion resistance of the steel.

4. When the Cu content in the steel increased from 0.4% to 1.1%, its corrosion resistance was not further improved. Therefore, 0.4% Cu is enough to improve the corrosion resistance of hot-rolled 301 ASS. The addition of Cu to 301 ASS does not improve the pitting resistance of the steel.

Author Contributions: Conceptualization, N.L.; writing—original draft preparation, N.L., H.Y. and X.W.; methodology, H.Y., X.W., L.X. and Y.Z.; validation, Y.L.; formal analysis, L.X. and Y.Z.; investigation, N.L.; resources, L.X., Y.Z. and Z.J.; data curation, N.L., H.Y. and X.W.; writing—review and editing, N.L. and Z.J.; supervision, Z.J.; project administration, N.L. and Z.J.; funding acquisition, L.X., Y.Z. and Z.J.; All authors have read and agreed to the published version of the manuscript.

Funding: This research was funded by [the National Natural Science Foundation of China] grant No. [52274338], [Doctoral Start-up Foundation of Liaoning] grant No. [2021-BS-243], and [Education Department Foundation of Liaoning Province] grant No. [LJKZ0303].

Data Availability Statement: All data generated or analysed during this study are included in this published article, and also, it is available from the corresponding author on reasonable request.

Conflicts of Interest: The authors declare that they have no conflicts of interest.

References

1. Mont Anstahl Special Profiles in Steel. Available online: <https://www.montanstahl.com> (accessed on 20 October 2022).
2. Stainless Structurals Asia. Available online: <https://www.montanstahl.com/contact/singapore> (accessed on 6 December 2022).
3. Li, S.; Zhang, L.; Zhao, O. Testing, modelling and design of hot-rolled stainless steel channel sections under combined compression and minor-axis bending moment. *Thin. Wall. Struct.* **2022**, *172*, 108836. [CrossRef]
4. Gardner, L. Stability and design of stainless steel structures—Review and outlook. *Thin. Wall. Struct.* **2019**, *141*, 208–216. [CrossRef]
5. Eskandari, M.; Najafizadeh, A.; Kermanpur, A.; Karimi, M. Potential application of nanocrystalline 301 austenitic stainless steel in lightweight vehicle structures. *Mater. Des.* **2009**, *30*, 3869–3872. [CrossRef]

6. Uksza, J.; Rumiński, M.; Ratuszek, W.; Blicharski, M. Texture evolution and variations of α -phase volume fraction in cold-rolled AISI 301 steel strip. *J. Mater. Process. Technol.* **2006**, *177*, 555–560. [[CrossRef](#)]
7. Li, N.; Jia, R.; Zhang, H.; Sha, W.; Li, Y.; Jiang, Z. In-situ Cu coating on steel surface after oxidizing at high temperature. *Materials* **2019**, *12*, 3536. [[CrossRef](#)]
8. Li, N.; Yan, L.; Wang, S.; Wang, C.; Zhang, H.; Ai, F.; Jiang, Z. Corrosion Behavior of Copper Bearing Steels and the Derived In-Situ Coating. *Metals* **2021**, *11*, 1462. [[CrossRef](#)]
9. Zhang, T.L.; Yu, H.; Li, Z.X.; Kou, S.; Kim, H.J.; Tillmann, W. Progress on effects of alloying elements on bainite formation and strength and toughness of high strength steel weld metal. *Mater. Res. Express.* **2021**, *8*, 032002. [[CrossRef](#)]
10. Wu, W.; Dai, Z.Y.; Liu, Z.Y.; Liu, C. Synergy of Cu and Sb to enhance the resistance of 3%Ni weathering steel to marine atmospheric corrosion. *Corros. Sci.* **2021**, *183*, 109353. [[CrossRef](#)]
11. Oguzie, E.E.; Li, J.B.; Liu, Y.Q.; Chen, D.M.; Li, Y.; Yang, K.; Wang, F.H. The effect of Cu addition on the electrochemical corrosion and passivation behavior of stainless steels. *Electrochim. Acta* **2010**, *55*, 5028–5035. [[CrossRef](#)]
12. Ujiro, T.; Satoh, S.; Staehle, R.W.; Smyrl, W.H. Effect of alloying Cu on the corrosion resistance of stainless steels in chloride media. *Corros. Sci.* **2001**, *43*, 2185–2200. [[CrossRef](#)]
13. Hermas, A.A.; Ogura, K.; Takagi, S.; Adachi, T. Effects of Alloying Additions on Corrosion and Passivation Behaviors of Type 304 Stainless Steel. *Corrosion* **1995**, *51*, 3–10. [[CrossRef](#)]
14. Pardo, A.; Merino, M.C.; Carboneras, M.; Coy, A.E.; Arrabal, R. Pitting corrosion behaviour of austenitic stainless steels with Cu and Sn additions. *Corros. Sci.* **2007**, *49*, 510–525. [[CrossRef](#)]
15. Li, B.B.; Qu, H.P.; Lang, Y.P.; Feng, H.Q.; Chen, Q.M.; Chen, H.T. Copper alloying content effect on pitting resistance of modified 00Cr20Ni18Mo6CuN super austenitic stainless steels. *Corros. Sci.* **2020**, *173*, 108791. [[CrossRef](#)]
16. Hou, Y.; Cai, S.; Sapanathan, T.; Dumon, A.; Rachik, M. Micromechanical modeling of the effect of phase distribution topology on the plastic behavior of dual-phase steels. *Comput. Mater. Sci.* **2019**, *158*, 243–254. [[CrossRef](#)]
17. Das, Y.B.; Forsey, A.N.; Simm, T.H.; Perkins, K.M.; Fitzpatrick, M.E.; Gungor, S.; Moat, R.J. In situ observation of strain and phase transformation in plastically deformed 301 austenitic stainless steel. *Mater. Des.* **2016**, *112*, 107–116. [[CrossRef](#)]
18. Xi, T.; Babar Shahzad, M.; Xu, D.; Zhao, J.; Yang, C.; Qi, M.; Yang, K. Copper precipitation behavior and mechanical properties of Cu-bearing 316L austenitic stainless steel: A comprehensive cross-correlation study. *Mater. Sci. Eng. A* **2016**, *675*, 243–252. [[CrossRef](#)]
19. Kim, K.W.; Park, S.J.; Moon, J.; Jang, J.H.; Kim, S.D. Characterization of microstructural evolution in austenitic Fe-Mn-Al-C lightweight steels with Cr content. *Mater. Charact.* **2020**, *170*, 110717. [[CrossRef](#)]
20. Wang, J.; Guo, W.; Sun, H.; Li, H.; Gou, H.; Zhang, J. Plastic deformation behaviors and hardening mechanism of M7C3 carbide. *Mater. Sci. Eng. A* **2016**, *662*, 88–94. [[CrossRef](#)]
21. Liu, Y.; Sun, Y. In-situ observation of interaction between precipitates and austenite during $\delta \rightarrow \gamma$ phase transformations. *Mater. Sci. Technol.* **2019**, *35*, 536–543. [[CrossRef](#)]
22. Curtze, S.; Kuokkala, V.T. Dependence of tensile deformation behavior of TWIP steels on stacking fault energy, temperature and strain rate. *Acta Mater.* **2010**, *58*, 5129–5141. [[CrossRef](#)]
23. Kim, B.; Lee, S.G.; Kim, D.W.; Jo, Y.H.; Bae, J.; Sohn, S.S.; Lee, S. Effects of Ni and Cu addition on cryogenic-temperature tensile and Charpy impact properties in austenitic 22Mn-0.45C-1Al steels. *J. Alloys Compd.* **2020**, *815*, 152407. [[CrossRef](#)]
24. Curtze, S.; Kuokkala, V.T.; Oikari, A.; Talonen, J.; Hänninen, H. Thermodynamic modeling of the stacking fault energy of austenitic steels. *Acta Mater.* **2011**, *59*, 1068–1076. [[CrossRef](#)]
25. Lee, S.; Kim, J.; Lee, S.J.; Cooman, B.C.D. Effect of Cu addition on the mechanical behavior of austenitic twinning-induced plasticity steel. *Scripta Mater.* **2011**, *65*, 1073–1076. [[CrossRef](#)]
26. Dong, Z.H.; Li, W.; Chai, G.C.; Vitos, L. Strong temperature -Dependence of Ni -alloying influence on the stacking fault energy in austenitic stainless steel. *Scripta Mater.* **2020**, *178*, 438–441. [[CrossRef](#)]
27. Remy, L.; Pineau, A. Twinning and strain-induced F.C.C. \rightarrow H.C.P. transformation in the Fe-Mn-Cr-C system. *Mater. Sci. Eng.* **1977**, *28*, 99–107. [[CrossRef](#)]
28. Yasnii, P.V.; Marushchak, P.O.; Hlad'ov, V.B.; Ya Baran, D. Correlation of the microdislocation parameters with the hardness of plastically deformed heat-resistant steels. *Mater. Sci.* **2008**, *44*, 194–200. [[CrossRef](#)]

Disclaimer/Publisher's Note: The statements, opinions and data contained in all publications are solely those of the individual author(s) and contributor(s) and not of MDPI and/or the editor(s). MDPI and/or the editor(s) disclaim responsibility for any injury to people or property resulting from any ideas, methods, instructions or products referred to in the content.